CHAPTER TWELVE

Drawability and Breaks

Contents

12.1. PRACTICAL DEFINITIONS

Drawability is the degree to which rod or wire can be reduced in cross section by drawing through successive dies of practical design. This is expressed in apparent true strain, $\varepsilon_t = \ln (A_0/A_1)$. Strictly speaking, such an expression should factor in redundant strain. However, this is rarely done in practice, although practical die designs and pass schedules do involve a moderate level of redundant work. Redundant work will generally reduce the possible drawing reduction, but no adjustment for this is usually made in drawability analysis unless Δ values are very high.

Wire Technology
ISBN 978-0-12-382092-1, DOI: 10.1016/B978-0-12-382092-1.00012-9

When drawing breaks occur at the die exit or at the capstan, the *drawability limit* has been reached. Drawability reflects a given metallurgical condition and *flaw* population. Typical flaws of importance are surface defects (crow's feet, drawn-in "dirt," etc.), and centerline defects (center bursts, porosity from solidification processing, etc.). Drawability may deteriorate with drawing and handling. It may be restored with the removal of cold work by annealing, although it must be understood that annealing will not eliminate flaws.

12.2. MEASURING AND ESTIMATING DRAWABILITY[77]

12.2.1 The role of the tensile test

Drawability may be evaluated with a tensile test, since tensile test fractures develop similar to certain drawing breaks. Figure 12.1 shows a schematic illustration of the manner in which porosity development at flaws or "fracture centers" limits area reduction in a tensile test.[78] With most wire materials, the most significant indicator of drawability from a tensile test is the *area reduction at fracture*. Fracture strain is often expressed as percent area reduction at fracture as shown in Equation 11.9:

$$\%\ \text{area reduction at fracture} = [1-(A_f/A_0)] \times 100, \tag{11.9}$$

where A_f is the cross-sectional area at fracture. However, it is better expressed as a true fracture strain, $\varepsilon_f = \ln (A_0/A_f)$. Very small values of A_f are especially important, and may require scanning electron microscopy (SEM) for meaningful measurement. On the other hand, metals of limited drawability may display quite limited reductions in area.

The most relevant measurements are those undertaken at the temperatures and strain rates of the drawing operation.

12.2.2 The Cockcroft and Latham workability criterion

From a metalworking research perspective, drawability is a special case of the more general concept of *workability*. Workability is the degree to which a material may be plastically deformed prior to fracture. Workability may be quantified by the Cockcroft and Latham fracture criterion.[79] The overall Cockcroft and Latham fracture criterion is given as follows:

$$\int_0^{\varepsilon_f} \sigma_o(\sigma^*/\sigma_o)\, d\varepsilon_o = c, \tag{12.1}$$

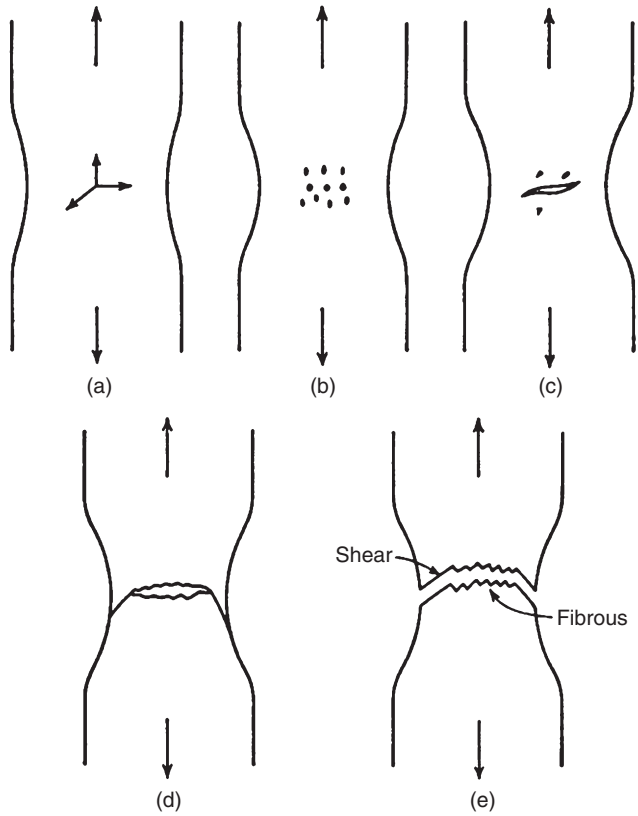

Figure 12.1 Schematic illustration of ductile fracture development in a tensile test. From G. E. Dieter, *Mechanical Metallurgy*, Third Edition, McGraw-Hill, Boston, MA, 1986, 262. Copyright held by McGraw-Hill Education, New York, USA.

where σ_o is effective stress, ε_o is effective strain; $(\sigma^\star/\sigma_o)$ is a dimensionless stress concentration factor representing the effect of the maximum tensile stress, $\sigma^\star$; and c is a material constant reflecting workability. It is understood that $\sigma^\star$ can only be positive in the integral, and that for purposes of integration, negative values of $\sigma^\star$ are replaced with a value of zero. Equation 12.1 reduces to

$$\int_0^{\varepsilon_f} \sigma^* \, d\varepsilon_o = c. \tag{12.2}$$

The rationale for this criterion can be explained as follows. First, resistance to fracture is toughness, and toughness can be expressed by the area under the effective stress-effective strain curve, or

$$\text{Toughness} = \int_0^{\varepsilon_f} \sigma_o \, d\varepsilon_o. \tag{12.3}$$

Second, it is assumed that pore growth, as illustrated in Figure 12.1, will not occur unless tension is present. Thus, "ductile damage" en route to fracture is only caused by the combination of plastic work *and* tension. Thus, Equation 12.3 is modified by the multiplier $(\sigma^\star/\sigma_o)$, with the further limitation that $\sigma^\star$ can only be positive in the integral, and that for purposes of integration, negative values of $\sigma^\star$ are replaced with a value of zero. Finally, the integration is complete when the fracture strain is reached, and the value of that integral is a measure of workability, equal to c.

Thus, the Cockcroft and Latham material constant, c, is a fundamental index of workability and drawability. It may be evaluated by way of the tensile test, since the true stress and true strain values of the tensile test are related to σ_o and ε_o, or to the effective stress and strain values, as discussed in Section 11.1.4.

Prior to necking, the value of σ_t in a tensile test is in fact $\sigma^\star$, and the value of ε_t is ε_o. Therefore up to that point the evaluation of the integral in Equation 12.2 is straightforward just like the area under the true stress-true strain curve. Beyond the point of necking, ε_t and ε_o must be evaluated as $\ln (A_0/A_1)$. Moreover, $\sigma^\star$ must reflect the radial tensile stresses in the neck, and must be calculated from a function describing the neck geometry. Figure 12.2 illustrates the distribution of $\sigma^\star$ in the neck cross section for two necking geometries. Therefore, the rigorous evaluation of the integral in Equation 12.2 is rather tedious.

Fortunately, the dominant aspect of the integral in Equation 12.2 is the true strain at fracture, or $\ln(A_0/A_f)$, which can vary widely among materials with diverse workabilities. In contrast, the average value of $\sigma^\star$ can be roughly approximated with the true stress at the point of necking, σ_{tu}, or

$$\sigma^*_{ave} \approx \sigma_{tu} = \sigma_{eu}(1 + \varepsilon_{eu}). \tag{12.4}$$

Therefore,

$$\int_0^{\varepsilon_f} \sigma^* \, d\varepsilon_o \approx (\sigma^*_{ave}) \ln(A_0/A_f) = \sigma_{eu}(1 + \varepsilon_{eu}) \ln(A_0/A_f) = c. \tag{12.5}$$

It is important to continue to note the dominant influence of $\ln(A_0/A_f)$ in Equation 12.5. In this context, it may be expedient to use $\ln(A_0/A_f)$ as the relative or comparative measure of workability and drawability.

As a predictor of drawability, $\ln(A_0/A_f)$ is most useful when the condition limiting drawability exists throughout the entire cross section, or when

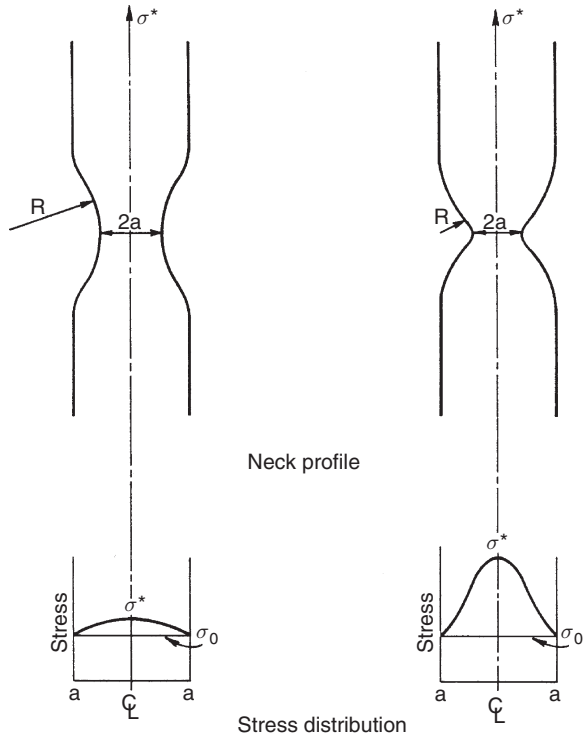

Figure 12.2 The distribution of the maximum tensile stress, σ*, in the neck cross section, for two necking geometries. From Thomas A. Kircher, Evaluation and Comparison of Workability for Two Limited-Workability Steels, M.S. Thesis, Rensselaer Polytechnic Institute, 1985.

it is at the centerline. Centerline weakness can result from casting porosity, alloy element concentrations, and newly forming center bursts.

12.2.3 Evaluating workability at the rod surface

When drawability is limited by surface conditions, such as crow's feet, oxide, rolled-in "dirt" and fines, twist tests and bend tests may be better indicators of drawability. This is because twist and bend tests maximize the strain at the rod or wire surface, leading to fracture development and drawability inference at the surface.

12.2.4 Evaluating workability with bending tests

Equation 11.16 leads to the bending fracture strain expression

$$\varepsilon_f \approx 1/[1 + (D/d)_{min}], \tag{12.6}$$

where $(D/d)_{min}$ is the smallest ratio of mandrel diameter to wire diameter that can be used without fracture. Clearly, one can subject wire to bending and wrap tests, infer the fracture strain, and use the fracture strain value as an indicator of drawability.

12.2.5 Evaluating workability with twist tests

Equation 11.22 leads to the twisting fracture strain expression

$$\gamma_f \approx \pi d\, N_{tmax}/L, \tag{12.7}$$

where N_{tmax} is the maximum number of twists that can be administered to the wire without fracture. Clearly, one can subject wire to twist tests, infer the fracture strain, and use the fracture strain value as an indicator of drawability.

12.2.6 Compression testing and the criterion of Lee and Kuhn[80]

While the problematical aspects of compression testing have been noted in Section 11.6.1, compression tests have been developed for careful analysis of workability at the surface. The pertinent compression test geometry is illustrated in Figure 12.3. The surface strains are described in terms of coordinates in the axial direction, h, and the circumferential direction, s. Thus, upon plastic deformation, the axial compressive strain, ε_z, is $\ln(h/h_0)$

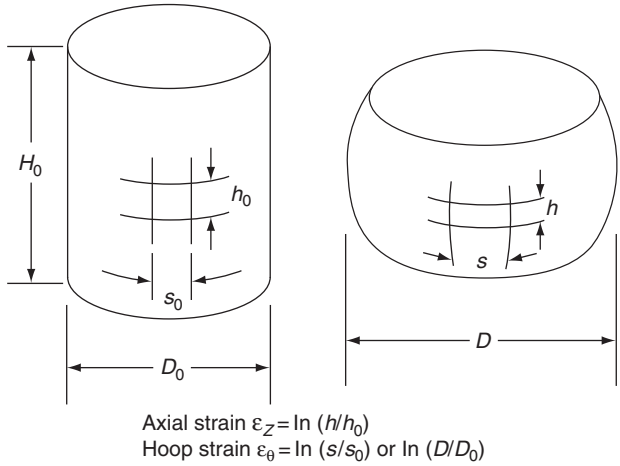

Figure 12.3 Geometry for workability testing in compression. From P. W. Lee and H. A. Kuhn, *Workability Testing Techniques*, G. E. Dieter Editor, American Society for Metals, Metals Park, OH, USA, 1984, 49. Copyright held by ASM International, Materials Park, OH.

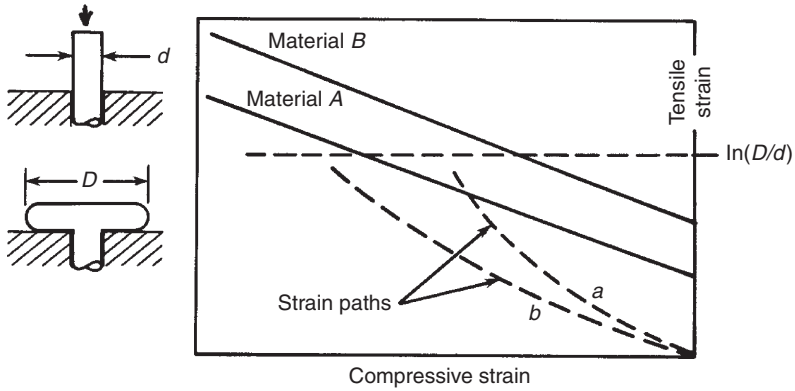

Figure 12.4 Geometry for workability testing in compression. From P. W. Lee and H. A. Kuhn, *Workability Testing Techniques*, G. E. Dieter Editor, American Society for Metals, Metals Park, OH, USA, 1984, 49. Copyright held by ASM International, Materials Park, OH.

and the circumferential tensile strain, ε_θ, is $\ln(s/s_0)$ or $\ln(D/D_0)$, where h_0 and h are starting and as-deformed axial direction dimensions, s_0 and s are starting and as-deformed circumferential direction dimensions, and D_0 and D are starting and as-deformed diameter maximums. Measurement of h and s values may be facilitated with a grid established (such as by etching) on the specimen surface.

Figure 12.4 displays ε_θ versus ε_z relationships for tests a (Material A) and b (Material B), up to a circumferential strain of ln(D/d). If the surface strains simply reflected uniform deformation, or equal values of circumferential and radial strains, then the strain paths would have followed a straight line relating tensile strain to compressive strain. In general, however, at a certain stage of the compression, the radial strain becomes less than the circumferential strain, and a "flat area" begins to develop on the surface, leading to a condition approaching plane strain with ε_z and ε_θ as the only strains continuing to change. Thus strain paths a and b turn upward away from the straight line. This condition of "plastic instability" leads to fracture once the strain path has departed a critical distance from the straight line or has intersected the limits labeled Material A or Material B.

The fracture conditions just described are defined by the fracture criterion of Lee and Kuhn[80] namely:

$$\varepsilon_\theta + {}^1\!/_2\varepsilon_z = q, \tag{12.8}$$

where q is a material property reflecting workability of the surface material. The respective values of q for Material A and Material B are to be found at the intercept of the respective lines with the tensile strain axis.

Various test options exist to establish a database to determine the value q, including that implicit in the diagrams to the left in Figure 12.4.

12.3. CATEGORIZING DRAWING BREAKS

Any time the wire breaks it is a significant event, whether in relation to down time and lost production or to scrap generation and lost product. Moreover, a drawing break signifies that something is wrong with the wire or with the wire processing. In this context, *all drawing breaks should be subjected to real-time scrutiny and saved for analysis*. If nothing else, the operator should register an immediate opinion and related observations, and the wire break ends should be cut off and placed in a labeled envelope. With appropriate microscopic and macroscopic observations, drawing breaks can be categorized as follows.

12.3.1 Category one: Breaks that do not reflect general wire quality, or damage from passage through the die

It is important to single out breaks that have nothing basic to do with the wire quality or with the actual drawing operation. Common examples are

Breaks at obvious cuts or abrasions. A typical example is shown in Figure 12.5.

Breaks at welds. A typical example is shown in Figure 12.6.

Breaks reflecting wire route damage. These may include damage that occurs where a wire crosses over another wire on a capstan, or where abrasion results from contact with worn sheaves and guides.

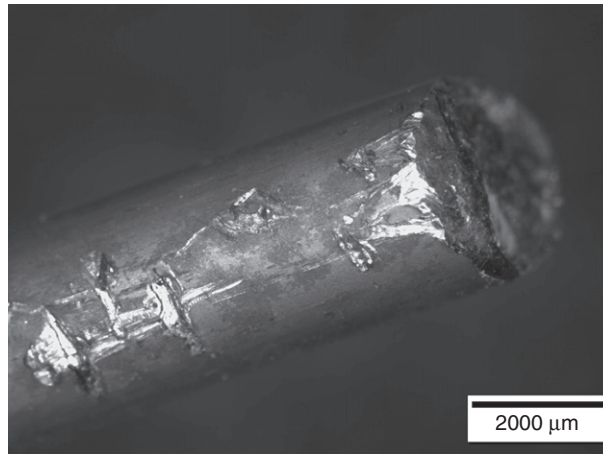

Figure 12.5 Typical example of a wire break at a cut or abrasion.

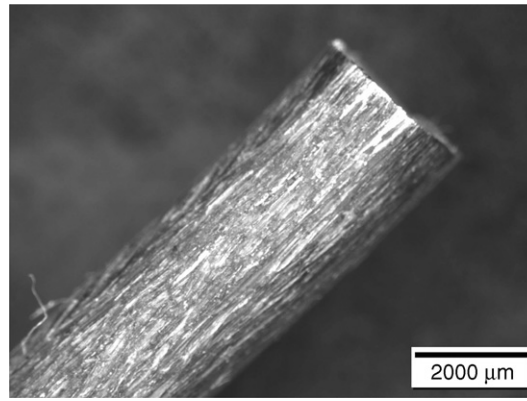

Figure 12.6 Typical example of a wire break at a weld. The longitudinal surface striations were generated in dressing the weld.

12.3.2 Category two: Breaks that primarily reflect mechanical conditions during passage through the die

The breaks in this category cannot be related to wire quality. They reflect solely the plastic flow of the wire in the die and the role of the lubricant. Common examples are

Wire tensile breaks due to a draw stress that exceeds the wire tensile strength. A typical example is shown in Figure 12.7.

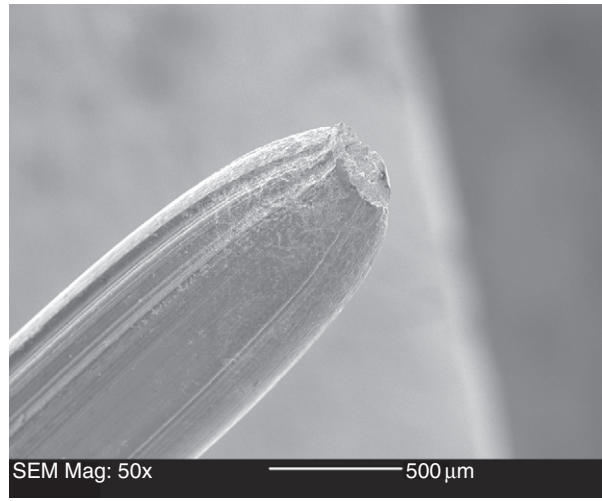

Figure 12.7 Typical example of a wire tensile break. From E. H. Chia and O. J. Tassi, Wire Breaks — Causes and Characteristics, Nonferrous Wire Handbook, Vol. 2, The Wire Association, Inc., Guilford, CT, 1981, 60.

Figure 12.8 Typical example of a wire break due to a center burst. Note "cup" on left, and "core" on right. (Courtesy of Horace Pops)

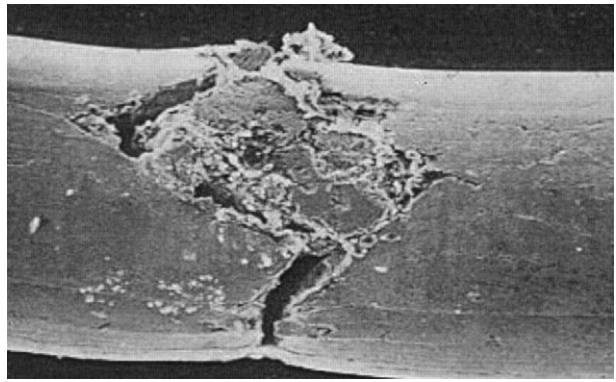

Figure 12.9 Typical example of a wire break due to a surface inclusion. (Courtesy of Horace Pops)

b. Breaks due to center bursts ("cuppy core" breaks). A typical example is shown in Figure 12.8.

c. Breaks due to crow's feet. Such a scenario is shown schematically in Figure 8.16.

12.3.3 Category three: Breaks where metallurgical or microstructural flaws in the wire greatly accelerate development of category two breaks

These breaks reflect the quality of the wire being drawn, and the role of wire flaws is directly evident in the fractography or morphology of the break. Generally such flaws occur at the wire center, where they exacerbate

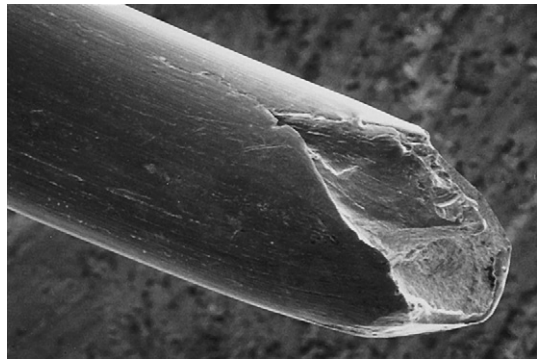

Figure 12.10 Example of an "inclusion absent break" in copper wire, where it is likely that a steel inclusion has fallen out. (Courtesy of Horace Pops)

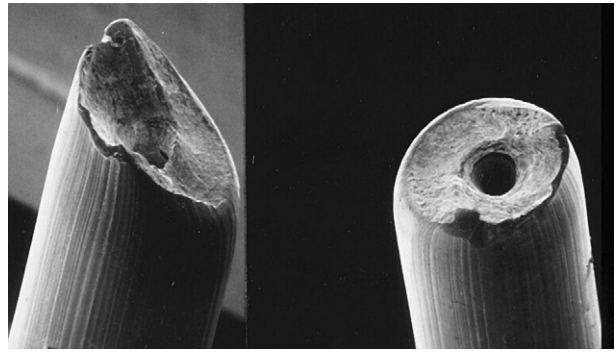

Figure 12.11 Example of an wire break due to macroporosity at the wire centerline. (Courtesy of Horace Pops)

the development of center bursts, or on the wire surface where they complicate friction and surface flow. Common examples are shown in Figures 12.9, 12.10 and 12.11.

12.4. MECHANICS OF DRAWING BREAKS[81]

12.4.1 The ratio of draw stress to flow stress

In the simplest concept of drawing, a break occurs when the draw stress equals the yield and/or breaking stress of the wire at the die exit. Yielding and breaking are generally associated because of the instability created by the plastic stretching of the wire between dies. Such a break is called a tensile break, since the conditions for failure in a tensile test are largely reproduced.

For practical analyses, we will utilize Equation 5.13:

$$\sigma_d/\sigma_a = \Sigma = [(3.2/\Delta) + 0.9](\alpha + \mu), \tag{5.13}$$

and take the position that when σ_d/σ_a, or Σ, equals one, the tensile break condition is essentially satisfied. At this point, vibrations, inertial loads, and lubricant fluctuations can be expected to put the draw stress "over the top" as far as yielding and fracture are concerned.

It is important to note that back stress, σ_b, can add significantly to the value of Σ. Equation 5.20 can be modified to display this role:

$$\sigma_d/\sigma_a = \Sigma = [(3.2/\Delta) + 0.9](\alpha + \mu) + \sigma_b[1-(\mu r/\alpha)(1-r)^{-1}]. \tag{12.9}$$

It should also be noted that relatively brittle wires may actually break on contact with the capstan where the tensile bending stress adds to the drawing stress. For a wire of diameter d, and a capstan of diameter D, the bending strain at the wire surface is given by $1/(1 + D/d)$, or about d/D when d is much smaller than D. Such bending tensile strains of 0.1% will add substantially to the local surface stress on the as-drawn wire. Wire crossovers are especially threatening in this regard.

12.4.2 Breaks without obvious flaws

Despite the simplistic criterion of Section 12.4.1, it is observed that breaks become intolerably frequent at values of Σ below one, even in wire without obvious flaws. In laboratory operations, or with certain highly controlled industrial situations, a Σ value as high as 0.9 may be tolerable. It is common in high productivity operations to have a Σ value of 0.7 cited as the practical maximum to avoid widespread flaw growth and frequent breakage.[82] Lower Σ maxima will be required in the face of a discernable flaw population.

Equation 5.13 can be used to project maximum reductions consistent with a Σ value of 0.7 for given values of die semi-angle and coefficient of friction. Such reductions are listed in Table 12.1. It is apparent in Table 12.1 that there is only a small effect of die angle on maximum drawing reduction. This observation must be tempered, however, with the understanding that α and μ are not necessarily independent. Die angle reductions can improve lubrication under thick film conditions, and can increase friction when lubrication is marginal.

Friction plays a major role in determining the maximum reduction, however. Table 12.1 indicates that thick film lubrication conditions (μ in the range of 0.03) may permit drawing reductions as high as 40% without frequent breaks. However, bright drawing conditions (μ in the

Table 12.1 Maximum reductions, as a function of die semi-angle and friction coefficient, for a draw-stress-to-average-flow-stress ratio of 0.7.

Die Semi-Angle (°)	Friction Coefficient	Maximum Reduction (%)
4	0.03	41
4	0.10	25
4	0.15	18
6	0.03	43
6	0.10	28
6	0.15	22
8	0.03	43%
8	0.10	30
8	0.15	23
10	0.03	42
10	0.10	30
10	0.15	24

range of 0.10) and marginal lubrication (μ in the range of 0.15) restrict drawing reductions to the 25–30% and 18–24% ranges, respectively.

In this context, a sudden increase in drawing break frequency may reflect increased friction, especially if no flaw population is apparent. As discussed in Chapter 8, such a deterioration in lubrication should be confirmable by microscopy.

12.4.3 Breaks in the presence of obvious flaws

The Σ limit of 0.7, in the absence of obvious flaws, reflects the fact that ductile fracture mechanics models predict the growth of even very small flaws at Σ values above this level. Very small inclusions are largely unavoidable, and even natural, such as copper oxides in ETP copper (see Chapter 13). Moreover, the initiation of center bursts and crow's feet leads directly to a developable flaw. Poor quality wire and poor drawing practice can present flaw sizes that grow at Σ levels well below 0.7. Such flaws include cuts, abrasions, and weld deterioration.

When flaw cross-sectional area, A_{fl}, becomes, for example, within an order of magnitude of the wire cross section, A, it is useful to examine the *net section stress*, σ_{ns}. The net section stress is the stress value obtained by dividing the force, F, by the cross-sectional area ($A - A_{fl}$) that remains when the flaw area is subtracted from the nominal wire cross section ($\pi d^2/4$). That is,

$$\sigma_{ns} = F/(A - A_{fl}) = (F/A)[A/(A - A_{fl})] = \sigma_d/(1 - A_{fl}/A). \qquad (12.10)$$

As an example, if a flaw were 20% of the cross-sectional area of the wire, then $\sigma_{ns} = \sigma_d/(1 \quad 0.2) = 1.25\ \sigma_d$.

Since it has been hypothesized that any flaw will grow when Σ or (σ_d/σ_a) exceeds 0.7, we can take the position that any flaw will grow when σ_{ns}/σ_a exceeds 0.7. If we replace σ_a with (σ_d/Σ), flaw growth is predicted when $\Sigma(\sigma_{ns}/\sigma_d)$ is at least 0.7. Replacing the stresses with force and area values, one obtains

$$(A_{fl}/A) = 1-\Sigma/(0.7), \tag{12.11}$$

where (A_{fl}/A) is the relative flaw size that is predicted to grow rapidly at a given Σ or (σ_d/σ_a) level. As a check for consistency, we can note that if the flaw is infinitesimal, and (A_{fl}/A) is zero, then the given value of Σ for flaw growth is 0.7, which is the (σ_d/σ_a) ratio at which we have said that even infinitesimal flaws will grow.

12.4.4 The case of ultra-fine wire drawing[83]

The production of ultra-fine wire (diameters the order of 0.02 mm) is grossly inhibited by the threat of breaks, and the associated loss of very-high-value-added wire. A number of measures are introduced to reduce breaks including screening of redraw rod; decrease in per pass reduction; reduction in drawing speed; use of carefully matched, low angle dies; rigorous lubricant maintenance and control; and intensive drawing machine oversight. Metzler has summarized these measures.[84]

In this context, the break frequency can be been modeled as:

$$B/L \approx A_{fl}\ N_{fl}\ J\ \Sigma, \tag{12.12}$$

where B/L is the number of breaks per unit length of wire, N_{fl} is the number of flaws per unit volume, and J is a fracture index inversely related to wire toughness. Common wire drawing experience suggests that J has a value in the range of four for metal of high toughness, and a value in the range of eight for average toughness. Much higher J values represent brittle wire. Ultra-fine copper wire drawing practice expectations indicate, by way of Equation 12.12, that a cubic meter of very high drawability copper rod should contain and/or develop no more than the order of fifty drawing-break-related flaws.

It is worth noting that Equation 12.12 seems to imply that B/L is independent of wire diameter. This would seem unreasonable given the great increase in break frequency often observed with continued drawing to

finer sizes. This increased B/L is accounted for by increases in the values of J, N_{fl}, and A_{fl} with progressive drawing reduction.

Although Equation 12.12 is presented for application to the case of ultra-fine-wire drawing, it can be usefully applied to heavier gage drawing practice. The roles of Σ and A_{fl} remain pertinent, even if N_{fl} requirements are less strenuous.

12.5. THE GENERATION OF "FINES"

During most drawing operations, the surface of the wire undergoes "wear" (wire wear as opposed to die wear), and small pieces of the wire (called "fines") flake off. Such behavior is included in this chapter, since it represents a local form of wire fracture. Figure 12.12 shows an example of an incipient fine in the act of emerging from a copper wire surface.[85]

The fines are involved with surface quality, since their formation leaves rough areas, and since the fines may be pressed into the drawn wire surface. Fines compromise lubrication and metal flow by clogging dies and by chemically reacting with the lubricant.

Gross fine development may reflect poor rod surface quality. Fine development can also reflect factors such as die angle and die alignment. Figure 12.13 shows a relationship of copper fine development to die angle, indicating that an intermediate, 16° included die angle minimizes fine development.[85] Such intermediate die angles are the norm in copper

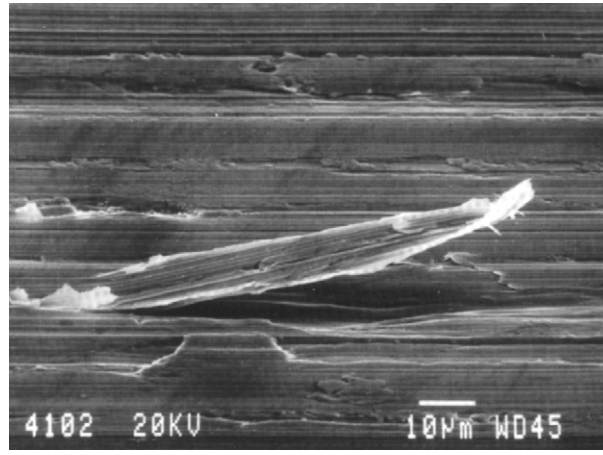

Figure 12.12 An incipient "fine," in the act of emerging from a copper wire surface. From G. J. Baker, Workpiece Wear Mechanisms in the Drawing of Copper Wire, Ph.D. Thesis, Rensselaer Polytechnic Institute, 1994.

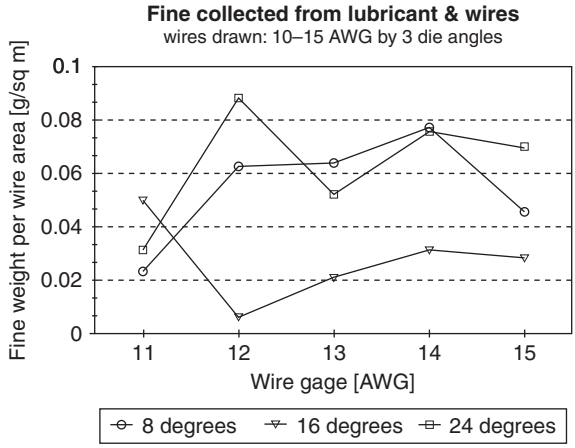

Figure 12.13 Relationship of copper "fine" development to drawing die angle. From G. J. Baker, Workpiece Wear Mechanisms in the Drawing of Copper Wire, Ph.D. Thesis, Rensselaer Polytechnic Institute, 1994.

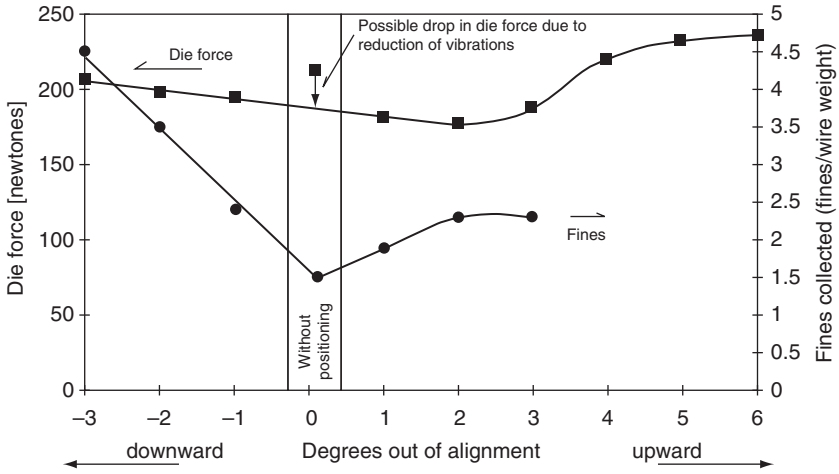

Figure 12.14 Data showing the minimization of copper "fine" development with good die alignment. From G. Baker and H. Pops, *Some New Concepts in Drawing Analysis of Copper Wire, Metallurgy, Processing and Applications of Metal Wires*, H. G. Paris and D. K. Kim (Eds.), The Minerals, Metals and Materials Society, Warrendale, PA, 1996, 29. Copyright held by The Minerals, Metals and Materials Society, Warrendale, PA, USA.

drawing, despite the general advantages often cited for low angle, low Δ drawing passes. Figure 12.14 shows a minimization of fine development with good die alignment.[86]

12.6. QUESTIONS AND PROBLEMS

12.6.1 A rod displays an ultimate tensile strength of 200 MPa, a uniform elongation of 17%, and an area reduction at fracture of 45%. Evaluate the workability constant, c, for the Cockcroft and Latham criterion.

Answer: Equation 12.5 can be used. For a 45% reduction, $\ln(A_0/A_f) = 0.60$, therefore the value of c is 140 MPa.

12.6.2 A low-flaw-content wire is drawn with a die with a 12° included angle. It is found that the maximum practical reduction, without excessive breaks, is 30%. Estimate the coefficient of friction.

Answer: Equation 5.13 can be used with the assumption that σ_d/σ_a can be 0.7. Putting in the values (do not forget the semi-angle) leads to a coefficient of friction of 0.089.

12.6.3 A 2 mm diameter wire has consistent flaws the size of 0.5 mm. What is the largest ratio of drawing stress to average flow stress that can be taken without probable breakage?

Answer: Equation 12.11 can be used, and the ratio (A_{fl}/A) can be approximated by the square of the diameter ratio. On this basis, σ_d/σ_a is estimated at 0.66. This is a high value and is probably only reasonable for a smooth-surfaced pore. Lower figures would probably result with solid, rough-surfaced inclusions.

12.6.4 Consider that the wire in Problem 12.6.3 is quite tough, but that the number of flaws considered to be present is 1000 per m^3. How many breaks per unit length can be expected with respective drawing-stress-to-average-flow-stress ratios of 0.5, 0.4, and 0.3?

Answer: Using Equation 12.12, estimating A_{fl} at $(0.5\,\text{mm})^2$ and inserting values, the relation $B/L = 10^{-3}\,(\sigma_d/\sigma_a)$ is calculated. The values of B/L are 0.0005, 0.0004, and 0.0003 for the respective (σ_d/σ_a) values of 0.5, 0.4, and 0.3. These values correspond to 2000, 2500, and 3000 meters per break.